DART: A Small-Scale Demonstrator for Rapid and Precise Rocket Payload Delivery

Brett Lougheed[1] and Nathan Tardy[2]
Florida Institute of Technology, Melbourne, Florida 32901, United States

Current suborbital cargo delivery methods are slow and may not respond well to time-sensitive situations. At the same time, while orbital launch vehicles are capable of high speeds, their single-use tendency drives prohibitive costs. In June 2021, to address this dilemma, the United States Air Force announced the fourth Vanguard program (Rocket Cargo), which aims to examine the possibility and practicality of using large commercial rockets for Department of Defense global logistics. Derived from the Rocket Cargo Vanguard program, the DART project is a 2024-2025 senior design initiative at the Florida Institute of Technology that aims to develop a small-scale, proof-of-concept demonstrator exploring the feasibility of using rocket propulsion for precise, point-to-point payload delivery. This work involves designing, building, and launching a model rocket to an altitude of at least 75 meters (~250 feet), carrying a payload of at least 75 grams (5% of the rocket's mass), and propulsively landing at a pre-determined landing zone no less than 50 meters (~165 feet) from the launch site. Technical aspects include leveraging additive manufacturing to support complex component geometries, performing rigorous trajectory simulation, and implementing a custom, fully autonomous control system capable of handling all flight operations. The project's success would serve a twofold purpose. First, it would fill a void of current propulsive landing projects at Florida Tech. More importantly, it would expand on the University's existing amateur rocketry knowledge base and present a smaller, more accessible model to test future thrust-vector-control and GNC systems.

I. Nomenclature

α_0 = Initial angle of attack [degrees]
α_1 = Peak angle of attack selected after α_0 [degrees]
C_{L_α} = Lift coefficient derivative [1/rad]
C_{m_α} = Moment coefficient derivative [1/rad]
C_{m_q} = Pitch damping coefficient [1/(rad/s)]
C_2 = Pitch differential equation $\dot{\theta}$ coefficient [kg-m^2/s]
D = Logarithmic decrement variable [1/s]
D_{ref} = Reference length (rocket tube diameter) [m]
t_0 = Initial time [s]
t_1 = Time of selected peak α_1 [s]
I_{zz} = Mass moment of inertia (MOI) about z axis [kg-m^2]
q_∞ = Freestream dynamic pressure [Pa]
SM = Static margin [unitless]
S_{ref} = Reference area (rocket tube frontal area) [m^2]
V_∞ = Freestream velocity [m/s]
X_{CG} = Distance to center of gravity from tip of nose cone [m]
X_{CP} = Distance to center of pressure from tip of nose cone [m]

[1] Project Manager, Aerospace Engineering Undergraduate Student, Department of Aerospace, Physics, and Space Sciences, AIAA Student Member (1585151)
[2] Systems Engineer, Aerospace Engineering Undergraduate Student, Department of Aerospace, Physics, and Space Sciences, AIAA Student Member (1401603)

II. Introduction

The fourth Vanguard program, Rocket Cargo, was announced by the United States Air Force (USAF) in June 2021 and aims to leverage emerging rocket technologies to provide a solution for delivering time-sensitive payloads anywhere across the globe in under one hour [1]. Such capability would not only be a significant asset for Department of Defense global logistics but would also enhance the United States Government's ability to rapidly respond to natural disasters and other humanitarian crises. Looking past the geopolitical difficulties inherent with implementing the Rocket Cargo program on a worldwide scale, realizing the technology to bring it to fruition poses multifaceted technical challenges worth exploring.

Stemming from the Rocket Cargo Vanguard program, the DART (Demonstrator for Autonomous Rapid Transport) project is a 2024-2025 aerospace engineering capstone design project at the Florida Institute of Technology. The project's highest-level goal is to demonstrate the practicality of using rocket propulsion for precise, point-to-point payload delivery, albeit at a much smaller scale than envisioned for Rocket Cargo. This work involves designing and building a reusable rocket capable of launching and propulsively landing, designing and implementing a control system capable of autonomously operating the rocket during flight and landing, and designing the rocket to integrate and fly with a payload of at least 5% of the rocket's total mass.

To ensure regulatory compliance while minimizing the barriers for testing, the rocket must comply with the Title 14 Code of Federal Regulations (CFR) Part 101.22 definition of a Class 1 amateur rocket, which includes limiting the rocket's total mass to no greater than 1500 grams as well as limiting the mass of all propellant in the rocket to no more than 125 grams [2]. In the same vein, the rocket must comply with the Title 14 CFR Part 101.23 general operating limitations of amateur rockets [3]. While the latter did not prove overly restrictive during the design process, the same cannot be said of the former, as will be discussed.

This work will overview key design and analysis aspects of the project, results of preliminary testing, and will conclude with a discussion of planned forward work. Emphasis is placed on the structural design of the rocket, as well as the results of structural and aerodynamic analyses necessary to verify the design against project requirements. As an integral component of the vehicle assembly, the avionics design will also be detailed, which includes the amalgamation of commercial-off-the-shelf (COTS) components with a custom printed circuit board. Lastly, flight simulation efforts will be discussed in the context of requirements verification and controller design.

III. Structural Design & Analysis

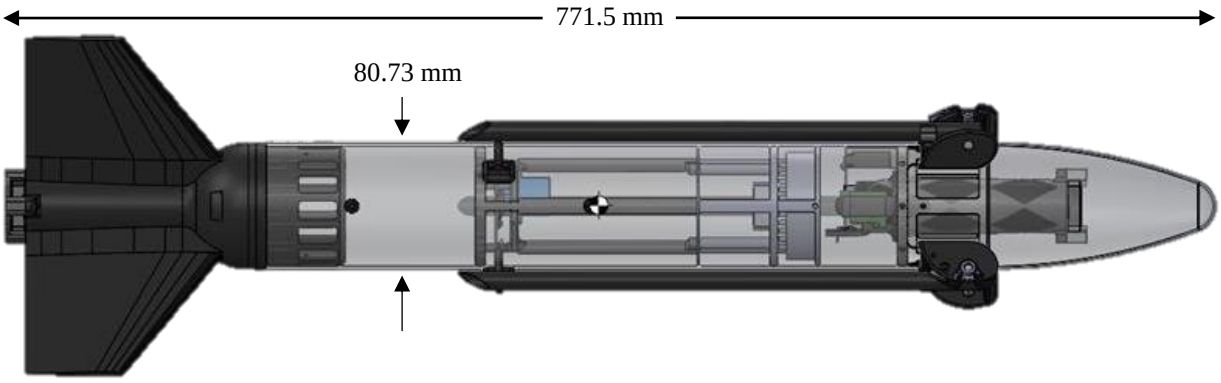

Fig. 1 System Design

The structural design of the DART rocket integrates three subsystems (controls, propulsion, and structures) while maintaining compliance with the constraints of the mass budget and system requirements. The vehicle's airframe is constructed from cardboard as a compromise between reducing mass, providing the strength required for launch and landing, and complying with structural requirements. The airframe diameter was selected to accommodate the propulsion system, recovery system, and interior mounting structure (IMS), which includes the avionics and payload bay. The structure ensures that the propulsion components are securely mounted and critical subsystems are housed without compromising vehicle integrity during the stresses of flight. To facilitate the vehicle's reusability and optimize mass efficiency, non-essential metal parts are minimized, adhering to the constraints set forth in the structures requirements.

A significant design challenge was ensuring aerodynamic stability during all flight phases. The rear-mounted fins provide passive stability during ascent and unpowered descent, preventing any undesirable pitching or yawing. As part of the vehicle's descent system, the thrust-vector-control (TVC) mechanism, located at the front, provides active control by gimbaling the descent motor to control both the rocket's attitude and velocity during the powered descent flight phase. This TVC mechanism is integrated into the vehicle's forward structure, ensuring that it functions independently of the ascent motor while maintaining control throughout the descent. The descent motor and TVC mechanism are housed in a design that allows the rocket to land on its nose, a departure from traditional designs where landing typically occurs tail-first. This configuration ensures that the thrust vector from the descent motor is directed for precise control while allowing the rocket to naturally pitch over during flight and accumulate lateral displacement placed at the aft end of the vehicle.

Thermal analyses were conducted on the TVC mechanism (Fig. 2) and ascent motor mount (Fig. 4) to ensure these components could withstand the conditions during launch and powered descent. The thermal load on the TVC mechanism during static fire tests was modeled, and results indicated that the gimbal system could withstand the expected thermal gradients without yielding. Similarly, the ascent motor mount, designed to secure the motor during the high-thrust ascent phase, was analyzed for thermal deformation and stress concentrations. The results confirmed that the selected materials could handle the heat generated during the motor's operation, ensuring a secure and stable mounting for the motor. This thermal analysis was essential in preventing structural failure during high-stress phases, particularly during ignition and thrust buildup.

The landing system, another critical structural element, includes landing legs designed to absorb the impact forces during touchdown. The legs are coupled with ratcheting hinges and a servo-actuated landing leg release mechanism that ensures they deploy at the optimal time during descent. The landing leg hinges include a ratcheting gear and pawl with a torsion spring that all integrate into a 3D printed spring hinge mount (Fig. 3).

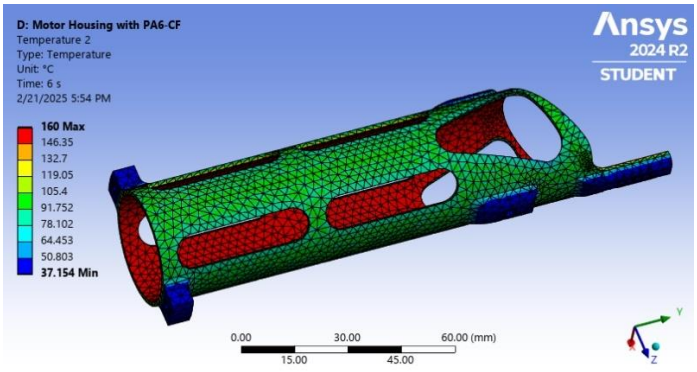

Fig. 2 TVC Motor Housing Thermal Analysis Results (Material: PA6-CF, Deflection Temperature: 183 C)

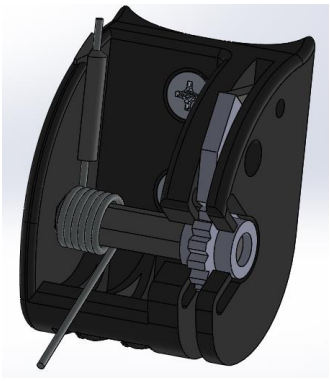

Fig. 3 Landing Leg Hinge

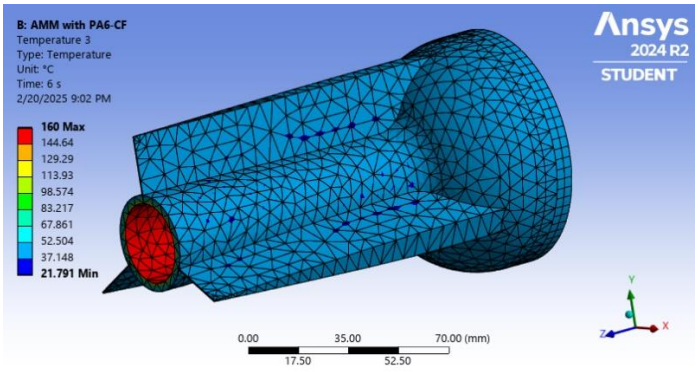

Fig. 4 Ascent Motor Mount Thermal Analysis Results (Material: PA6-CF, Deflection Temperature: 183 C)

Fig. 5 Landing Leg Release Mechanism (Deployed Configuration)

The release mechanism (Fig. 5) ensures that the landing legs are deployed reliably and at the appropriate moment of the descent to prevent premature activation. The legs themselves were engineered with sufficient strength to absorb the forces of landing without damaging the rocket, while also maintaining a low mass to meet the vehicle's

stringent mass budget requirements. This design has undergone continuous refinement to balance reliability with minimal weight, addressing considerations such as material fatigue and structural integrity under varying conditions. The structural analysis of the landing legs confirms their ability to absorb shock forces effectively, ensuring the vehicle remains stable and upright upon landing.

The nose cone of the DART rocket (Fig. 6) is another key structural component, designed with a unique shoulder to fit around the mounting hardware of the landing leg hinges. The shape of the nose cone follows a spherically blunted ogive design with a 2:1 length to diameter ratio, which is effective in minimizing drag during ascent. This shape allows for smooth airflow over the vehicle, reducing the risk of aerodynamic instability. The nose cone also houses the TVC, which, as previously discussed, is essential for the vehicle's autonomous operation.

Fig. 6 Nose Cone Design

Finite element analysis (FEA) was instrumental in validating the structural integrity of the rocket. The FEA simulations focused on areas that would experience high forces during flight, which included the TVC mechanism and the ascent motor mount. These simulations indicated that while the TVC mechanism could endure the expected loads, some minor deformation occurred, which was addressed through design improvements that increased the mechanism's rigidity by approximately 30%. This was particularly critical in ensuring the TVC system could effectively control the descent motor's gimbal without failure, and stress results of the final design are shown in Fig. 7. Furthermore, the ascent motor mount's design underwent rigorous analysis to verify it could withstand the high thrust loads generated during powered ascent (Fig. 8), ensuring the rocket remained stable and operational during the entire flight phase.

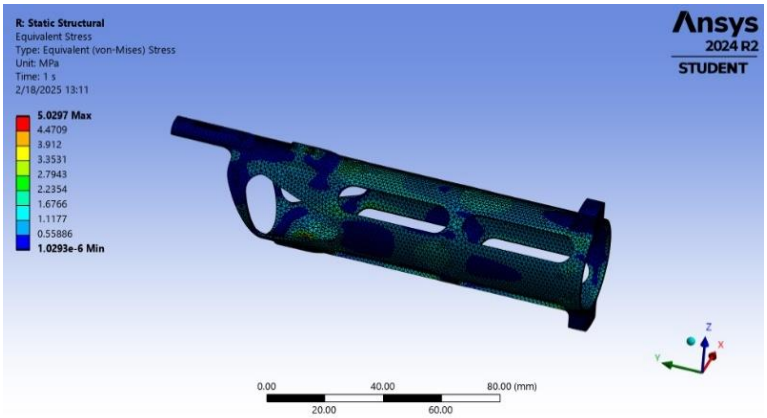

Fig. 7 TVC Motor Housing Structural Analysis Results (Equivalent Stress – Material: PA6-CF, Yield Stress: 102 MPa)

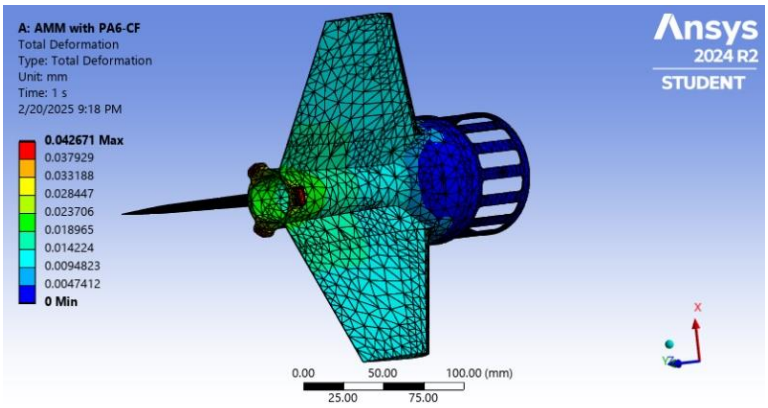

Fig. 8 Ascent Motor Mount Structural Analysis Results (Deformation – Material: PA6-CF)

The structural design of the DART rocket is characterized by careful material selection, scrupulous thermal and structural analyses, and a modular integration of key subsystems. The airframe, ascent motor mount, TVC mechanism, and landing legs were all meticulously designed to deliver a balance between performance, safety, and reusability. The vehicle's structure meets the project's requirements, ensuring the rocket can withstand the conditions of launch, flight, and landing while maintaining its ability to deliver payloads with high precision.

IV. Aerodynamics Analysis

Ansys Fluent computational fluid dynamics (CFD) analyses were leveraged to confirm the rocket's design complied with the project's requirements for both static[3] and dynamic[4] stability as well as to increase the accuracy of the flight simulation.

To ensure the design was statically stable, static Ansys Fluent analyses were performed with the SST k-ω viscous model utilizing a free-stream velocity of 32 m/s (the maximum expected). An average of 246,000 mesh elements were used in a 2 m x 2 m x 4.5 m control volume (Fig. 9). The rocket's angle of attack was varied from -45 degrees to 45 degrees, and for each instance, the lift, drag, and moment acting on the rocket were recorded. A coupled pressure velocity scheme was utilized (Fig. 10), which allowed force and moment values to converge within 100 iterations. These results were then used to calculate the rocket's moment coefficient as a function of the angle of attack. As shown in Fig. 11, for attack angles on the closed interval [-0.5, 0.5] radians (-28.6 degrees to 28.6 degrees), the derivative of the moment coefficient with respect to angle of attack is negative. This indicates a restorative moment, which satisfies the criteria for positive static stability.

To further verify the oscillations induced by the restoring moment would dampen over time, transient dynamic mesh analyses were conducted with 400 time steps of 0.01 seconds each and 150 iterations per time step, the results of which are shown in Fig. 12. Starting from a 45-deg disturbance, the attack angle diminishes to within 10-deg after about 2 seconds. While a shorter settling time would be preferable, the results observed are the result of a small static margin (1.07, illustrated in Fig. 13) that was induced by the unconventional geometry shown in Fig. 1. The dynamic results were approximated as a 2nd

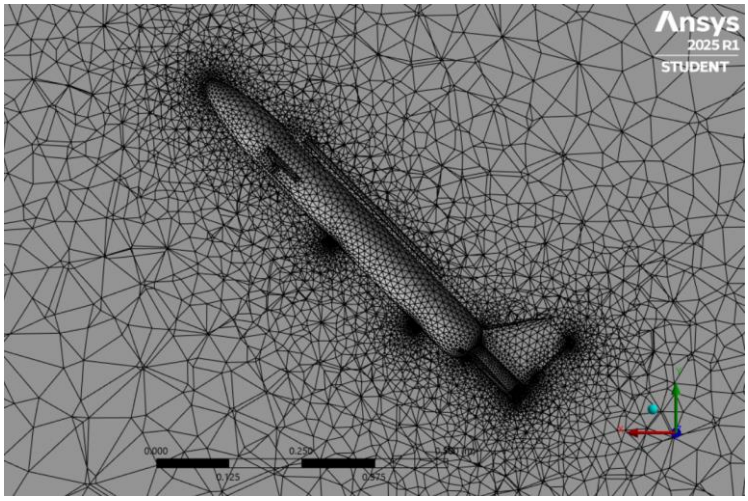

Fig. 9 Ascent Geometry Meshing

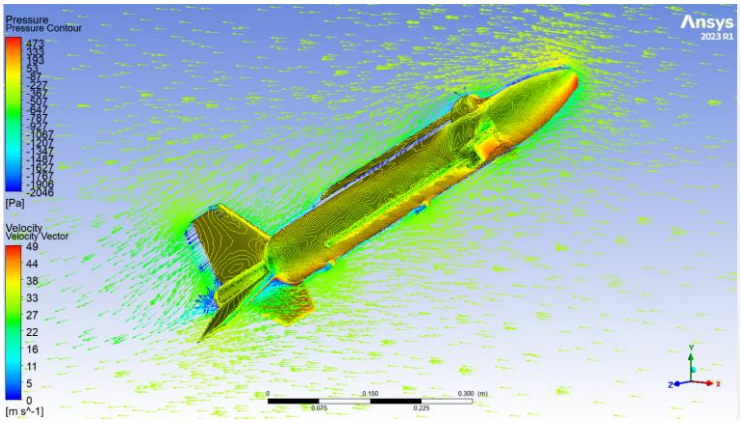

Fig. 10 Coupled Pressure Velocity Scheme

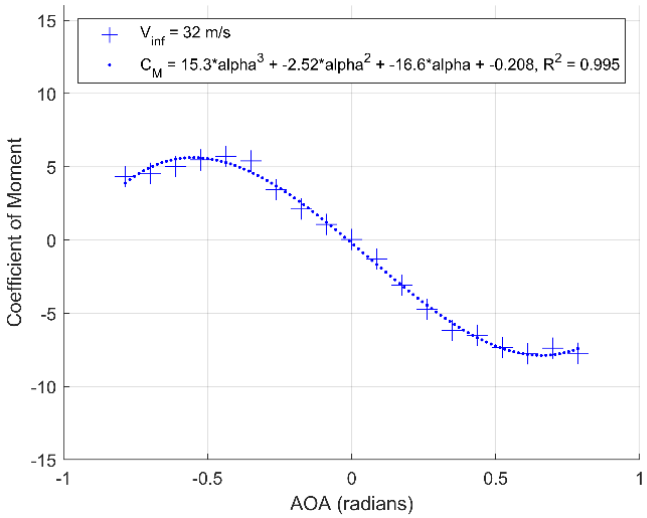

Fig. 11 Moment Coefficient vs Attack Angle [rad]

[3] AERO.01: During all flight phases, the rocket shall maintain positive longitudinal static stability.
[4] AERO.02: During all flight phases, the rocket shall maintain positive longitudinal dynamic stability.

order underdamped differential equation. A logarithmic decrement method [4] was used to calculate C_{m_q} as

$$D = \frac{\ln\left(\frac{\alpha_1}{\alpha_0}\right)}{t_1 - t_0}$$

$$C_2 = 2 \cdot I_{zz} \cdot D$$

$$C_{m_q} = -\frac{C_2}{\frac{q_\infty}{I_{zz}} \cdot S_{ref} \cdot D_{ref}},$$

whereas the static results were used to approximate the pitch damping coefficient [5] using the static margin:

$$SM = \frac{X_{CP} - X_{CG}}{D_{ref}}$$

$$C_{m_q} = -\left(C_{L_\alpha}\right)(SM)^2 \left(\frac{D_{ref}}{V_\infty}\right).$$

The values obtained for the pitch damping coefficient (-0.0246 [1/(rad/s)] from the dynamic analysis and -0.0244 [1/(rad/s)] from the approximations reliant on the static analysis results) agreed within 1% and were less than zero, which was sufficient to satisfy the requirement for dynamic stability. With the requirements satisfied, the static analysis results were implemented in the flight simulation software (as the trendlines fitted to the generated data) to define the aerodynamics for the entire rocket. This eliminated reliance on the Barrowman equations, which are the conventional method for calculating the aerodynamic forces on the rocket's exterior components but are limitedly predicated on assumptions that would have been invalid to apply to the DART rocket's design.

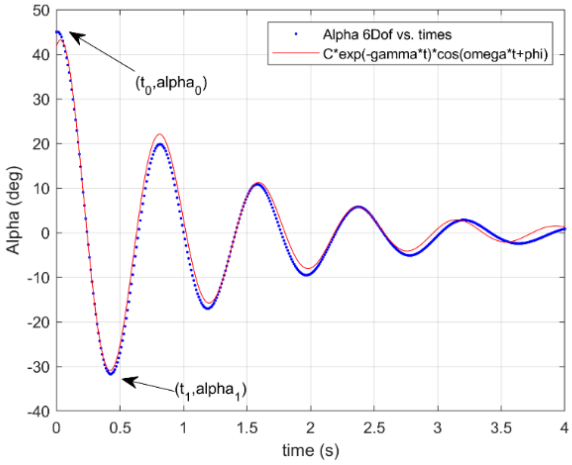

Fig. 12 Attack Angle [deg] vs Time [s]

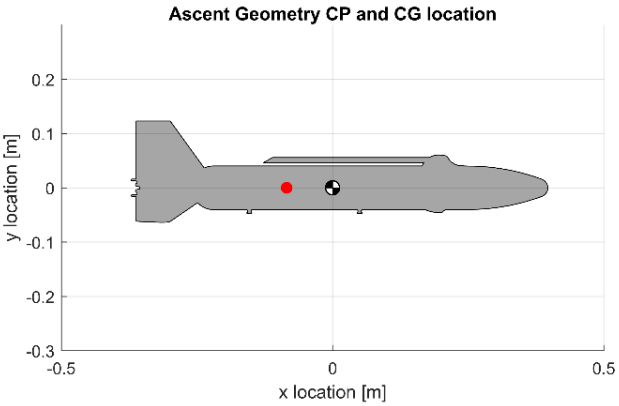

Fig. 13 Illustration of Ascent Configuration CG (Checkered) and CP (Red) Locations

V. Avionics Design

The avionics system of the DART rocket plays a crucial role in ensuring the vehicle's autonomy and control throughout its flight. At the core of the avionics system is the flight computer, which processes data from various sensors, executes control algorithms, and manages critical tasks such as abort handling and propulsion control. The flight computer is integrated with a custom-designed printed circuit board (PCB), which houses the microcontroller, sensor interfaces, communication modules, and data storage systems. These components are essential for the rocket's operation, as they allow for accurate state estimation, precise control, and reliable communication with the ground station.

The barometer is used to measure atmospheric pressure, providing vital data for estimating altitude during the rocket's ascent and descent phases, fulfilling controls requirement CTL.01[5]. The inertial measurement unit (IMU) is responsible for sensing linear accelerations and rocket orientation, critical for real-time trajectory tracking and attitude control, addressing the requirements CTL.02 and CTL.03[6]. The GPS module interfaces with the avionics to supply

[5] CTL.01: During all flight phases, the flight computer shall sense barometric pressure real-time.
[6] CTL.02-03: During all flight phases, the flight computer shall sense linear accelerations and rocket orientation real-time.

global positioning, which is essential for navigation and trajectory monitoring, satisfying CTL.05.[7] These sensors work together to provide the flight computer with accurate information on the rocket's state, enabling it to perform necessary control actions such as adjusting the TVC mechanism and activating the abort system if needed.

The microcontroller serves as the central processing unit, handling all sensor data and executing control algorithms. It processes input from the barometer, IMU, and GPS and uses this data to control various systems, including the descent motor ignition and parachute deployment. The XBee radio enables communication with the ground station, allowing for manual abort commands and real-time telemetry data, fulfilling CTL.06.[8] For post-flight data analysis, the SD card provides a storage medium to log all flight data, as required by CTL.04.[9] The TVC header pins are incorporated into the PCB to facilitate communication with the TVC system, ensuring that the rocket can maintain proper attitude during controlled descent, meeting controls requirements CTL.08 and CTL.09.[10] Additionally, servo headers are included to control the deployment of the landing legs and other mechanical actuators, addressing CTL.07.[11]

The final PCB design follows a dual-sided layout to maximize space efficiency while keeping the avionics package compact for horizontal integration. The IMU is centrally located with the pyro channels for the descent motor and abort system, barometer, and landing leg release servo header surrounding it (Fig. 14). On the other side of the board (Fig. 15), the microcontroller and other components, such as the sensors and communication modules, are positioned to minimize interference and ensure optimal signal routing. This design allows the avionics to function reliably during all phases of the flight, from launch to landing. The board is engineered to withstand the conditions of rocket flight, including vibrations, and the high acceleration forces experienced during launch.

The PCB schematic (Fig. 14 and Fig. 15) illustrates the integration of all these components. The layout ensures adequate power distribution to maintain consistent operation throughout the mission. The power management system is designed to provide stable voltage levels to all components, factoring in the dynamic conditions of flight.

Fig. 14 Top of Flight Computer

Fig. 15 Bottom of Flight Computer

VI. Flight Simulation

Considerable effort was dedicated to the integration of the design with a six degree-of-freedom (6DOF) flight simulation software, with the primary objectives of trajectory planning and controller tuning. While conventional model rockets can be accurately simulated with COTS software such as *OpenRocket*, *RASAero*, and *RockSim*, the DART rocket's irregular configuration demanded an alternative solution. Initially, the rocket's mass and aerodynamic characteristics were accumulated and used to simulate the trajectory via a custom state-derivative function compatible with a MATLAB numerical integrator (ODE45). While the state-derivative function leveraged the well-documented 6DOF equations of motion for a missile presented in [6], even with making gross simplifications of the rocket's aerodynamics and the local atmospheric conditions, it required substantial effort to achieve meaningful results.

[7] CTL.05: On measuring a deviation from the domain of nominal trajectories, the control system shall trigger an in-flight abort.
[8] CTL.06: On receiving the abort signal from the ground station, the control system shall trigger an in-flight abort.
[9] CTL.04: After landing, the control system shall write flight data to a storage medium within 5 seconds.
[10] CTL.08-09: The control system shall limit the vertical landing velocity to no more than 1 meter per second and the horizontal velocity to no more than 0.5 meters per second.
[11] CTL.07: The control system shall deploy the landing legs no less than 1.5 seconds before landing.

Accordingly, the simulation work pivoted to utilize the Python-based rocket trajectory simulation library *RocketPy*, which advertises as "the next-generation trajectory simulation solution for High-Power Rocketry" and entered the arena of trajectory simulation software circa 2021 [7]. It uses a class-based architecture that enables the creation of "Motor," "Rocket," "Environment," and "Flight" objects (among others), which retain the information about the rocket's motor, the rocket itself, the geographical and atmospheric conditions of the launch site, and the simulated flight, respectively. To define the launch site environment, *RocketPy* defaults to using the International Standard Atmosphere (ISA), which excludes any wind information, but provides the mechanisms to pull weather data from sources including "the European Centre for Medium-Range Weather Fore-casts (ECMWF), the Canadian Meteorological Centre (CMC), and the National Oceanic and Atmospheric Administration (NOAA)" [8].

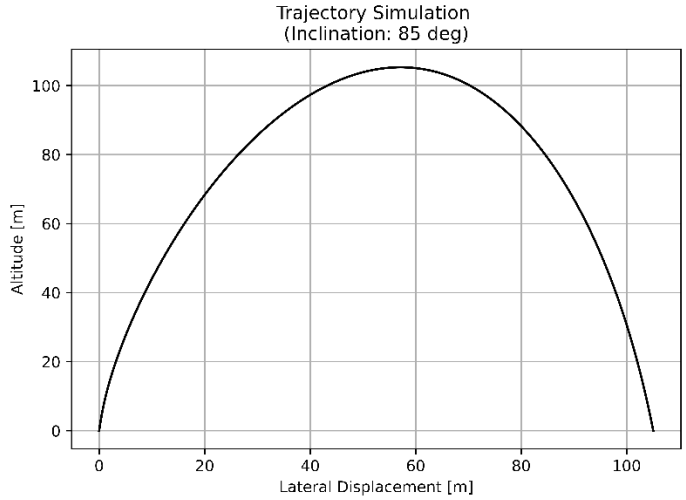

Fig. 16 Altitude [m] vs Lateral Displacement [m]

RocketPy trajectory simulation results indicate the rocket is expected to reach an apogee of roughly 114 meters when launched purely vertical and in the absence of wind. After reducing the launch inclination to 85 degrees (5 degrees from vertical), the rocket achieves both an apogee and a lateral displacement of over 100 meters, as shown in Fig. 16. This simulation uses the measured thrust curve discussed in section VII, indicating the motor contains sufficient impulse to deliver the rocket to the minimum apogee and lateral displacement specified by the project requirements.

Since the rocket is required to land within a pre-determined landing zone, *RocketPy* was also used to obtain the launch parameters (inclination and heading) corresponding to the optimal trajectory[12], an example of which is illustrated in Fig. 17. This optimal trajectory then served as the baseline to generate the domain of nominal trajectories (DNT), more thoroughly described as the flight envelope representing all trajectories that will lead the rocket to impact the ground within the landing zone.

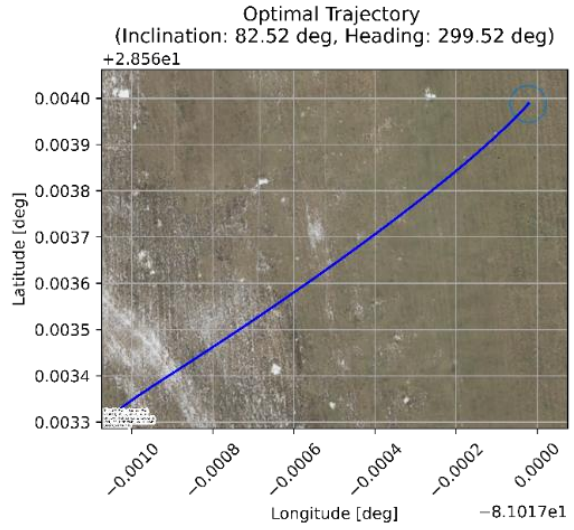

Fig. 17 Example Optimal Trajectory

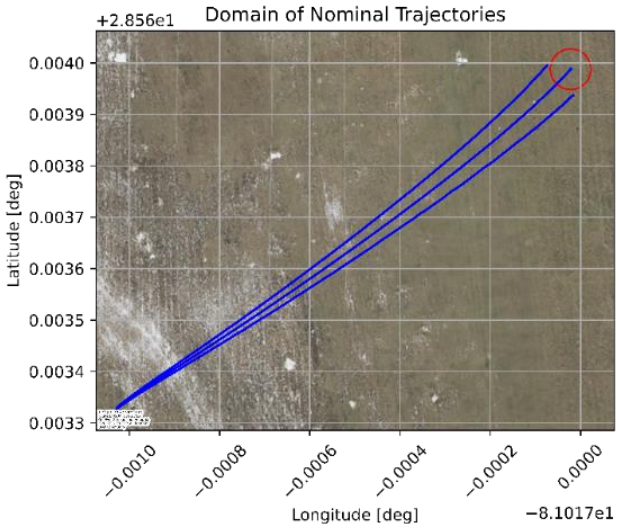

Fig. 18 Example Domain of Nominal Trajectories

[12] The optimal trajectory is defined as the trajectory for which the rocket will impact the ground in the center of the landing zone.

The DNT corresponding to the example optimal trajectory is shown in Fig. 18. For safety, the flight computer will implement a custom software method to monitor the rocket's position against the DNT boundaries and will deploy the parachute if it determines the rocket has exited the DNT[13]. This is a requirement of the flight software necessitated by project requirements; the functionality of the software method has been verified via Monte Carlo simulation, in which the launch inclination and heading were sampled from random uniform distributions centered at the respective optimal values and with ranges of ± 1 deg. The results of the Monte Carlo simulation are shown in Fig. 19, in which the green trajectories are those that remained within the DNT and the red trajectories are those that departed the DNT (and thus required an in-flight abort). For the red trajectories, there is evidence of the parachute deployment events in the unique geometry of the trajectories, which is a by-product of the rocket drifting with the wind as it descends under the parachute. In all, the simulated control system behavior, which is based on the same algorithm that will be implemented on the flight computer, satisfies the project's applicable controls requirements.

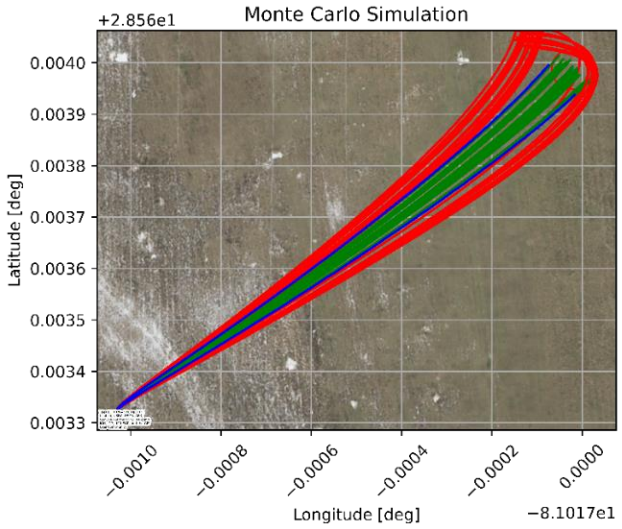

Fig. 19 Monte Carlo Simulation Results

As the flight simulation progresses, it will expand to include the powered descent flight phase, which involves simulating the TVC mechanism's effect on the (coupled) translational and rotational motion of the rocket. This will come hand-in-hand with the development of the TVC algorithm, to be further discussed in section VIII.

VII. Preliminary Testing

The preliminary testing phase for the DART project has been critical in validating key components of the rocket and ensuring they meet the project's design and performance requirements. The completed tests, which include Static Fire Test 1, Static Fire Test 2, and the Abort System Test, have provided valuable data to support the design decisions made in the Preliminary Design Review and Critical Design Review. These tests were instrumental in verifying the functionality of the propulsion system, TVC mechanism, and abort recovery system, which are essential to achieving the vehicle's mission of propulsive landing and payload delivery.

Static Fire Test 1 was conducted to characterize the performance of the AeroTech G25W solid rocket motor, used for both the ascent and descent propulsion systems. The primary objective of this test was to obtain a thrust curve for the motor and to measure the timing delay between the ignition command and the commencement of measurable thrust. The experimental thrust curve obtained from this test, shown in blue in Fig. 20, is implemented in the flight simulation to ensure the motor provides enough impulse to deliver the rocket to the minimum apogee and lateral displacement specified by the project's propulsion requirements[14]. The test successfully measured the motor's thrust profile, which matched closely with the expected values from [9], shown in red in Fig. 20. Additionally, the test measured the ignition delay, which was found to be 675 milliseconds. This information is crucial for calibrating the flight software and ensuring that the motor timing is optimized for the vehicle's controlled descent.

[13] To minimize the chances of damaging flight hardware, as well as to ensure the parachute is not deployed while the motor is firing, the flight computer will wait until at or after apogee to deploy the parachute if it senses a departure from the DNT.

[14] PROP.04-05: The APS shall provide sufficient impulse to deliver the rocket to an apogee of at least 75 meters and a lateral displacement of at least 50 meters.

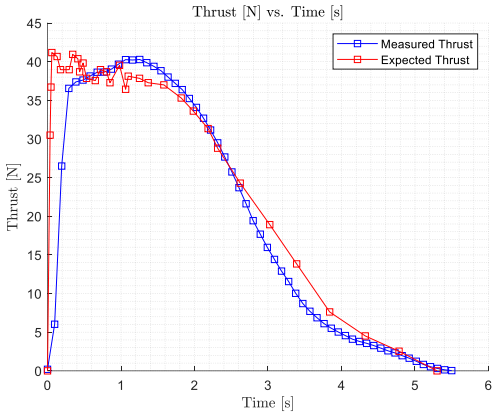

Fig. 20 Measured Thrust [N] vs Time [s]

Static Fire Test 2 focused on validating the TVC mechanism, which is integral to the rocket's descent phase. This test aimed to measure the gimbal angle of the motor during the static fire and verify the performance of the TVC system. The test successfully demonstrated the functionality of the TVC mechanism by gimbaling the motor while firing the engine. The gimbal angle was visually verified using test videos to confirm the gimbal behavior was essentially identical to dry testing, despite the IMU disconnect preventing direct comparison with the commanded angle. Although the data was not obtained, the test still provided valuable insights for refining the control algorithms used in flight. An image from this test (Fig. 21) illustrates the TVC mechanism in action, showing the motor's movement and the level of control achieved during the gimbal test.

The Abort System Test was conducted to verify the functionality of the recovery system in the event of an in-flight abort. The test aimed to simulate an abort scenario and confirm that the flight computer could trigger parachute deployment when an abort signal was received. The test successfully demonstrated that the flight computer received the abort signal and activated the parachute deployment mechanism as intended. This test satisfied the requirements SYS.12[15] and CTL.06, ensuring that the rocket has a redundant safety mechanism for recovery in case of trajectory deviations or other failures.

The tests completed to date have not only verified the basic functionality of critical systems but have also provided a foundation for refining the flight software and control systems. These preliminary tests have validated the rocket's propulsion, control, and recovery mechanisms, ensuring that the systems are ready for more advanced testing phases. The data gathered from these tests will be used to confirm the vehicle's design and performance ahead of full vehicle testing and final flight demonstrations.

Fig. 21 TVC Mechanism Gimballed during Static Fire 2

VIII. Future Work

As discussed in section VI, flight simulation is largely complete with the exception of the powered descent phase. The first challenge presented with simulating this flight phase is correctly timing the ignition of the descent motor to minimize the rocket's landing velocity, which must meet performance thresholds specified in the project's controls requirements. Once the motor's ignition is timed correctly, the following step will involve implementing the TVC algorithm in the flight simulation, which is anticipated to use a linear-quadratic regulator (LQR) controller with control states including the rocket's vertical velocity, horizontal velocity, and attitude angle[16]. The control outputs will include the TVC gimbal angles as well as the command to deploy the landing legs.

For requirements verification, the remaining tests include an *Ascent Test* followed by the *Full Flight Tests*. The *Ascent Test* seeks to verify system requirement SYS.04[17] in addition to controls requirements CTL.01-03[18], and intended to corroborate the results of the flight simulation (discussed in section VI) that indicate the rocket is expected to attain the required minimum apogee. Additionally, this test will ensure the flight computer's data recording capability through all flight phases is comparable to pre-flight ground testing, which will become of critical importance moving into the *Full Flight Test* campaign, which relies on the recorded data from the flight computer as the primary mechanism for requirements verification.

[15] SYS.12: On reception of the abort signal, the rocket shall abort the flight.
[16] "Attitude angle" being defined as the angle between the rocket's orientation and the inertial X-Y plane (the ground).
[17] SYS.04: The rocket shall attain a minimum altitude of 75 meters.
[18] CTL.01-03: During all flight phases, the flight computer shall sense barometric pressure, linear accelerations, and rocket orientation parameters real-time.

Each *Full Flight Test* will be an opportunity to verify the functionality of all vehicle systems and satisfy the project's performance requirements. It is also expected that the data from the preliminary *Full Flight Tests* will help refine the controller algorithm to increase the chances of a successful controlled descent in subsequent flights.

IX. Conclusion

The DART project has made significant progress in advancing thrust-vector-controlled, reusable rocketry at the model-rocket scale. With the successful completion of key preliminary tests, core systems such as propulsion, TVC, and recovery have been validated. These tests have provided useful data to refine the rocket's design, ensuring all essential systems function for safe and precise flight. Moving forward, the DART project is on track to meet its objectives, and as a showcase of experimental methods, it seeks to contribute to the broader field of reusable rocketry by stimulating discussion of the technologies it demonstrates.

Acknowledgments

As stated in section II, this work has been the result of an undergraduate team effort accumulated over the course of more than a year. As such, the authors only take credit for a portion of the content presented herein; much attribution is owed to all members of the team, without which the project would not have achieved a fraction of its progress to-date. Specifically, the authors would like to acknowledge Luke Aagaard as the project's Aerodynamics Engineer, who conducted the CFD analyses and performed the data analysis discussed in section IV, Rylen Struthers as the Structures Lead, who coordinated the structural design effort and was largely responsible for the design of the landing system, and Jack O'Hara as a Controls Engineer, who leveraged prior electronics experience to spearhead the design of the flight computer and flight software. Additional, and no-less-important team members include: Kian Jamal as the Controls Lead, Jack Smith and Johann Vennink as Structures Engineers, Zuleyka Priscila Figueroa Pineda as the Propulsion Lead, and McKennah Vale as a Propulsion Engineer/Safety Lead.

Furthermore, the team would like to thank the project's faculty advisors, Dr. Firat Irmak and Dr. Darshan Yadav from the Florida Institute of Technology, in addition to Steven Holmberg as the project's Graduate Student Assistant, for their continuous guidance and technical expertise. In the same vein, the team expresses gratitude to the staff of the Florida Tech L3Harris Student Design Center, not only for serving as constant sources of support for manufacturing, but also for providing equipment and a productive work environment.

Lastly, the team recognizes AIAA at Florida Tech as an invaluable network for undergraduate students, and thanks the organization's executive board, as well as Dr. Danilo de Camargo Branco as the faculty advisor, for all the development opportunities they facilitate for the club's members.

References

[1] "The Air Force Wants to Drop 100 Tons of Cargo From Space," Popular Mechanics, Jun 04 2021. Retrieved 16 February 2025. https://www.popularmechanics.com/military/research/a36610555/air-force-rocket-cargo-concept/

[2] "14 CFR 101.22 -- Definitions." Retrieved 16 February 2025. https://www.ecfr.gov/current/title-14/part-101/section-101.22

[3] "14 CFR 101.23 -- General Operating Limitations." Retrieved 16 February 2025. https://www.ecfr.gov/current/title-14/part-101/section-101.23

[4] Mandell, G. K., Caporaso, G. J., and Bengen, W. P., "Topics in Advanced Model Rocketry," Cambridge, 1973.

[5] Whitmore, S., "Static and Dynamic Stability, Longitudinal Pitch Dynamics."

[6] "Defense Technical Information Center." Retrieved 20 February 2025. https://apps.dtic.mil/sti/citations/ADA151529

[7] "RocketPy Documentation — RocketPy 1.8.0 Documentation." Retrieved 20 February 2025. https://docs.rocketpy.org/en/latest/

[8] Ceotto, G. H., Schmitt, R. N., Alves, G. F., Pezente, L. A., and Carmo, B. S., "RocketPy: Six Degree-of-Freedom Rocket Trajectory Simulator," *Journal of Aerospace Engineering*, Vol. 34, No. 6, 2021, p. 04021093. https://doi.org/10.1061/(ASCE)AS.1943-5525.0001331

[9] "AeroTech G25W • ThrustCurve." Retrieved 3 March 2025. https://www.thrustcurve.org/motors/AeroTech/G25W/